Desalination and Water Treatment
www.deswater.com

doi: 10.5004/dwt.2019.23497

143 (2019) 148–157
March

A new approach to assessing the ageing process of strongly basic anion-exchange resins: preliminary research

Paweł Wiercik[a,*], Magdalena Domańska[a], Janusz Łomotowski[a], Magdalena Kuśnierz[a], Tomasz Konieczny[b]

[a]*Wrocław University of Environmental and Life Sciences, The Faculty of Environmental Engineering and Geodesy, Institute of Environmental Engineering, Grunwaldzki Square 24, 50-363 Wrocław, Poland, Tel. +48 71 320 10 38; email: pawel.wiercik@upwr.edu.pl (P. Wiercik), Tel. +48 71 320 55 53; email: magdalena.domanska@upwr.edu.pl (M. Domańska), Tel. +48 71 320 10 34; email: janusz.lomotowski@gmail.com (J. Łomotowski), Tel. +48 71 320 55 72; email: magdalena.kusnierz@upwr.edu.pl (M. Kuśnierz)*
[b]*Municipal Water and Sewage Company Wrocław, 14/16 Na Grobli St., 50-421 Wrocław, Poland, Tel. +48 71 340 95 00; email: tomasz.konieczny@mpwik.wroc.pl*

Received 16 May 2018; Accepted 20 November 2018

ABSTRACT

Fouling of the anion exchangers with organic compounds is a very common phenomenon. These compounds adsorb on the anion exchangers surfaces causing a decrease in the ion-exchange capacity. In practice, the performance of ion exchanger is generally assessed based on the breakthrough curves and the studies of the adsorption kinetics. There is little research in the literature concerning the surface changes of the resin beads. The image analysis enables recognition of the beads morphology, and Fourier-transform infrared (FTIR) spectroscopy enables detection of the foulants. To the authors' knowledge, the application of these methods is a new approach to the organic fouling phenomenon. In this paper, image and FTIR analyses as well as scanning electron microscopy (SEM) were applied to assess the ageing process of two strongly basic anion exchangers in the process of treating of effluent containing high concentration of nitrites and nitrates. Effluent from sludge derived from fermentation chambers, dewatered on filter presses, and subsequently subjected to biological and membrane processes was fed through anion exchangers. The image, SEM and FTIR analyses indicated the accumulation of humic acids, which remained on the beads surface after regeneration, causing changes in the beads shape from circular to more elongated.

Keywords: Image analysis; FTIR spectroscopy; SEM; Ageing process; Organic fouling; Anion-exchange resin

1. Introduction

The efficiency of ion exchange (IE) is largely influenced by the presence of certain additives or impurities in the solution, which may lead to resin fouling. The most important among them are colloidal additives, iron and manganese compounds, organic impurities, free chlorine and dissolved oxygen. Ion exchangers are sensitive to the presence of polar organic compounds in water because they can be irreversibly bound by the exchangers and consequently block capillaries and the functional groups of ion exchangers [1–3].

The organics are characterised by a broad range of molecular weights, overall negative charge due to the presence of the carboxyl and phenolic groups and the structure containing aromatic and aliphatic sub-structures [4–6]. The attraction of organics to the anion exchanger is nearly the same as for the sulfate ion, and the reaction between an organic compound and the surface of anion exchange resin occurs quickly. On the

* Corresponding author.

contrary, the penetration of an organic molecule inside the resin bead is slow due to its size [7]. Organics are mostly composed of humic substances, which are the polymers formed by a microbial decay of plant and animal residues and occurring widely in natural waters [3,8,9]. Humic substances in terms of their solubility in water are classified as: humic acids (HAs) (soluble in alkaline water solutions), fulvic acids (soluble in water, alkali, alcohols and mineral acids), ulmic acids (soluble in alcohols, e.g., ethanol) and humins and ulmins (insoluble) [10]. Fouling caused by the presence of organic compounds contributes to greater conductivity and lower pH of the filtrate, earlier ion exchanger breakthrough point, longer washing periods following regeneration and lower IE capacity [3]. Organic fouling is chiefly caused by soluble HAs, whose structure includes chloride or hydroxyl ions that are exchanged for mobile chloride, sulphate or hydroxyl ions connected with the functional groups of ion exchangers [3]. The resulting structures are accumulated on the surface of the ion-exchanger resin bead and block the diffusion of ions inside it. As a result the resin becomes hydrophobic, and its moisture decreases, as does its porosity and the IE capacity [3,11]. Such connections may become irreversible and result in the ineffectiveness of regeneration. Thus it is recommended to use polyacrylic resins, which are more resistant than the polystyrene ones due to larger hydrophilic structures that enable high-molecular organic compounds to penetrate the resin bead thanks to its aliphatic structure, and whose regeneration allows for the effective removal of organic compounds [3]. The second mechanism of organic fouling concerns physical adsorption between the hydrophobic moieties of organic molecule and the resin polymer [12]. Adsorption takes place mainly when weakly basic resins are applied and when the neutral fraction of organic matter is removed on strongly basic resins [13].

The performance of the ion exchanger is generally assessed based on breakthrough curves of different ions, pH, conductivity, turbidity, dissolved organic matter (DOM), etc. [14]. The comparison between a resin after being regenerated with a fresh one can also be used to assess the capacity loss of ion exchanger [3]. The capacity of the resin can be read from the titration curves and corresponds to the amount of sodium hydroxide that produces change in pH [15]. The adsorption performance of the resin can be determined by percolation of the solution containing analysed factor such as DOM, HA or specific ions in different concentration levels through separate IE columns [3,14]. The study of kinetics of the adsorption process is another possibility to describe the operation of an ion exchanger [11,16–18].

The organic fouling of the anion-exchange resins can be evaluated by means of the instrumental methods which are focused mainly on the detection and the quantitative determination of organic compounds. The reduction of the organics removal with the increase of regeneration number results from the increase of foulants on the resin surface [5,17,19,20]. The organic matter can be measured on a total organic carbon analyser, UV and UV–vis spectrophotometer (UV absorbance, UV_{254}), fluorescence spectrophotometer (DOM) or chromatograph. The last one is used to estimate the polarities and molecular weights of DOM [5,12]. There is little research in the literature concerning the analyses of the surface changes of the resin beads by means of scanning electron microscopy (SEM) and X-ray photoelectron spectroscopy (XPS). To the authors' knowledge, there is no literature on the application of image analysis and Fourier-transform infrared (FTIR) spectroscopy to study the resin beads surface, which are commonly used to assess the fouling of membranes during water and wastewater treatment [21–27]. Unfortunately SEM analysis, unlike FTIR spectroscopy, is not able to give information about the foulant species. Walker and Boyer [19] using SEM observed greater fouling of the resin regenerated with bicarbonate than chloride. Xiao et al. [28] detected microcracks on the resin beads resulted from the oxidising behaviour of Cr(VI). With the aid of XPS they examined the elemental composition of the resin surface and proved the oxidation of polymer matrix and functional groups of the resins. XPS can also be used to identify the foulants [28,29].

This preliminary study was intended to test whether the presently used measurement methods such as image analysis, SEM and FTIR spectroscopy can aid in determining the ageing process of the anion-exchange resins. In order to establish the ageing process of strongly basic anion-exchange resins, image analysis using the Malvern Morphologi G3SE analyser was performed. As a result it was possible to compare the beads of fresh, exhausted and regenerated resins in terms of various morphological parameters. The detection of the foulant was possible with the aid of FTIR spectroscopy. To the authors' knowledge, using FTIR spectroscopy and image analysis to recognise the morphology of the resin beads and to detect that the foulants is new approach to assess the ageing process of the ion exchangers. These methods supplement the knowledge on the ageing process and lead to a better understanding of its nature. The examination of the surface of the resin beads by means of FTIR spectroscopy and image analysis is quick and cost-effective. This is a new approach to the problem because in practice the loss of the IE capacity in anion exchangers is controlled by analysing the change in the amount of the removed anions per one unit of anion-exchange resin in the subsequent service cycles. The resin regeneration process was based on sodium bicarbonate. In literature on the subject there have been few investigations into the performance of sodium bicarbonate because in most cases chlorides or, alternatively, hydroxides were used. Chloride regeneration increases the risk of plumbing corrosion posed by waste brine and leads to increased salinity of the environment. Compared to chloride-form resins, its bicarbonate form is equally efficient in the removal of nitrates and sulphates from water while reducing the harmfulness of the resulting waste brine to people and ecosystems [30,31].

2. Materials and methods

The research was conducted with the use of Lewatit MonoPlus M 500 and Lewatit S 5428 anion exchangers produced by Lanxess (Germany). The former is a strongly basic, gel-type anion-exchange resin consisting of monodisperse beads based on a styrene–divinylbenzene copolymer, whose functional groups are quaternary amines. The Lewatit S 5428 anion exchanger is a strongly basic, macroporous anion-exchange resin based on a crosslinked polyacrylate. The characterisation of both anion exchangers is shown in Table 1.

To load the resins, effluent from sludge derived from a fermentation chamber and dewatered on filter presses on Janówek Wastewater Treatment Plant (WWTP) was used.

Fig. 1 depicts a fragment of the experimental stand situated at WWTP Janówek that was used in the research. Before being treated with the appropriate IE resin on the stand, the effluent was subjected to separate treatment during the processes of nitritation and nitrification in sequencing batch reactors, followed by microfiltration (MF) and nanofiltration (NF). Fig. 2 schematically outlines the conducted experiments. After the MF process, the nitrificated effluent was directed onto an NF membrane placed in a flat sheet module, and the obtained permeate was further treated in an IE column containing the Lewatit MonoPlus M 500 resin. Having passed the MF membrane, the nitritated effluent was then treated on an NF membrane placed in a spiral module, after which the permeate was fed through an IE column with the Lewatit S 5428 resin.

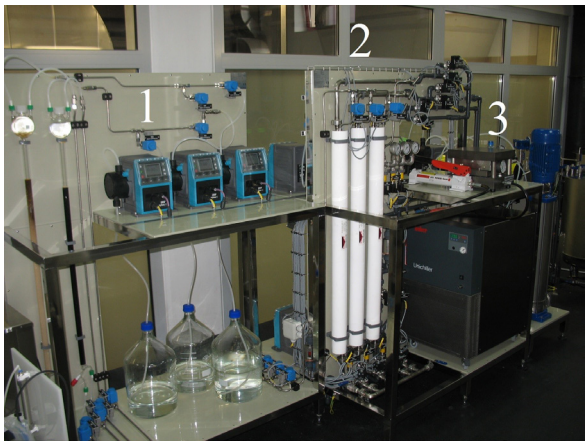

Fig. 1. (1) Ion-exchange system, nanofiltration modules with (2) spiral and (3) flat sheet membranes on the experimental stand in WWTP Janówek.

Ten IE cycles were conducted with the Lewatit MonoPlus M 500 resin and fifteen cycles with the Lewatit S 5428 resin. In each cycle the permeate after NF was fed through the IE column using a peristaltic pump. Samples of effluent from the columns were taken for physicochemical analysis every 24 min (1 L). In each cycle the IE process was conducted until the nitrate breakthrough point (in the case of tests with the Lewatit MonoPlus M 500 resin) or nitrite breakthrough point (tests with the Lewatit S 5428 resin).

The conducted experiments were supposed to show that under different conditions of the pretreatment and IE the organic fouling occurs (even after pretreatment on NF membranes) and the application of modern instrumental methods is suitable to describe the changes of the resins surface.

Beads of fresh, exhausted and regenerated (after the last cycle of anion exchange) resin were subject to image analysis with the Malvern Morphologi G3SE analyser with measurement range of 0.5–3,000 μm, SEM analysis and to FTIR analysis with the Thermo Scientific Nicolet iZ10 FT-IR spectrometer.

The Malvern Morphologi G3SE analyser provides information about the particle size distribution, their shapes and particle greyscale levels. The reports include all the registered particles together with their complete individual morphological parameters (diameter, width, length, surface area, perimeter, circularity, elongation, convexity, surface porosity, density, width to length ratio, etc.) [32].

Attenuated total reflection (ATR) FTIR analyses were performed using a Thermo Scientific Nicolet iZ10 FT-IR

Table 1
Properties and operation conditions of Lewatit MonoPlus M 500 and Lewatit S 5428 resins

	Lewatit Monoplus M 500	Lewatit S 5428
Matrix	Crosslinked polystyrene	Crosslinked polyacrylate
Structure	Gel	Macroporous
Functional groups	Quaternary amine, Type I	Quaternary amine, Type I
Commercial form	Cl^-	Cl^-
Appearance	Yellow, translucent	White, opaque
Mean bead size (mm)	0.61 (±0.05), minimum 90%	0.4–1.6, minimum 90%
Total capacity (minimum val/L)	1.2	0.85
Operating temperature (maximum °C)	70	80
Operating pH range	0–12	0–12

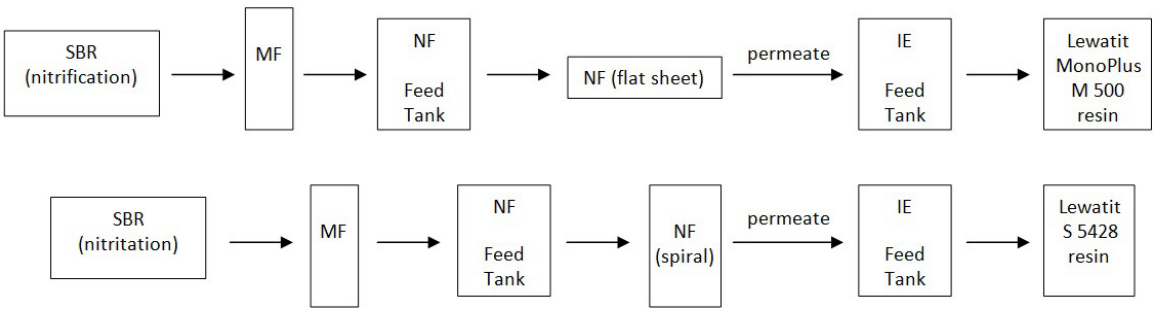

Fig. 2. Scheme of conducted experiments.

spectrometer, the module of Thermo Scientific Nicolet iN10 MX microscope equipped with Smart iTX accessory with diamond plate. Each spectrum of the resin bead is the average of 32 scans in the 400–4,000 cm^{-1} wavenumber range at 4 cm^{-1} spectral resolution.

The structure of the beads surface was analysed by SEM Zeiss Evo LS 15 (Zeiss, Oberkochen, Germany). Samples were coated with gold particles using a 300-s program (Edwards, Scancoat six, HHV Ltd., Crawley, UK) transferred to the microscope chamber, and observed using SE1 detector, at 10 kV of filament tension under high-vacuum conditions. Microphotographs were captured at 400× and 7,000× magnification.

Table 2
Chemical constitution of raw effluent from sludge dewatered on filter press

Parameter	Raw effluent
Ammonium (mg NH_4^+/L)	648.00
Nitrate (mg NO_3^-/L)	1.99
Nitrite (mg NO_2^-/L)	2.27
Conductivity (μS/cm)	2,789
pH (–)	8.80
Turbidity (NTU)	9.27
Sulphate (mg SO_4^{2-}/L)	154.70
Phosphate (mg PO_4^{3-}/L)	93.16
Chloride (mg Cl^-/L)	253.00
Alkalinity (mval/L)	27.20
Absorbance U_{254} (cm^{-1})	0.243

3. Results and discussion

The physicochemical constitution of raw effluent from sludge dewatered on filter press is presented in Table 2, whereas Tables 3 and 4 show the effluent after biological treatment (nitrification and nitration) and NF. The permeate obtained in the NF process was then fed into a steel tank with a capacity of 100 L, from which it was taken in the subsequent service cycles (the permeate after the NF process on a flat sheet or spiral membrane was fed into two different tanks). Storing the permeate in tanks significantly altered

Table 3
Chemical constitution of effluent after nitrification and nanofiltration on flat sheet membrane treated then with Lewatit MonoPlus M 500 resin

Parameter	Effluent after nitrification	Variability of NF permeate composition during whole research
Ammonium (mg NH_4^+/L)	0.116	NM
Nitrate (mg NO_3^-/L)	2,313	1,791–4,171
Nitrite (mg NO_2^-/L)	0.164	NM
Conductivity (μS/cm)	6,133	4,079–7,199
pH (–)	8.00	8.75–9.18
Turbidity (NTU)	5.55	0.22–40.23
Sulphate (mg SO_4^{2-}/L)	37.80	1.70–559.50
Phosphate (mg PO_4^{3-}/L)	411.44	10.24–709.96
Chloride (mg Cl^-/L)	204.00	176.00–391.00
Alkalinity (mval/L)	13	5–32
Absorbance U_{254} (cm^{-1})	0.161	0.02–0.142

NM, not measured.

Table 4
Chemical constitution of effluent after nitritation and nanofiltration on module with spiral membrane treated then with Lewatit S 5428 resin

Parameter	Effluent after nitritation	Variability of NF permeate composition during whole research
Ammonium (mg NH_4^+/L)	10.76	0.026–17.79
Nitrate (mg NO_3^-/L)	376.65	268.95–863.97
Nitrite (mg NO_2^-/L)	5,062	733.63–3,381
Conductivity (μS/cm)	6,157	3,098–4,209
pH (–)	7.80	7.70–9.90
Turbidity (NTU)	3.69	0.14–1.20
Sulphate (mg SO_4^{2-}/L)	107.80	118.50–954.50
Phosphate (mg PO_4^{3-}/L)	276.82	0.46–49.58
Chloride (mg Cl^-/L)	240.00	129.8–302.00
Alkalinity (mval/L)	28	7–15
Absorbance U_{254} (cm^{-1})	0.184	0.006–0.115

its constitution because of the occurrence of reduction and oxidation processes.

Subjecting the effluent to MF and NF did not eliminate organic compounds, which fouled both anion exchangers. Fig. 3 presents the Lewatit MonoPlus M 500 resin after five service cycles. A similar phenomenon occurred in the Lewatit S 5428 resin, albeit its extent was reduced due to greater resistance to organic fouling (Fig. 4).

During the IE process, the colour of the resin changed from light yellow to dark brown, and the change persisted after the regeneration process as well. The presence of organic compounds was indirectly proven by absorbance values with wave length of 254 nm (Tables 3 and 4). It resulted in a reduction of IE capacity (Figs. 5 and 6). The reduced IE capacity was also largely affected by the presence of sulphate, phosphate and chloride ions in the permeate.

Figs. 7 and 8 show SEM microphotographs of both types of anion exchanger at 400× and 7,000× magnification,

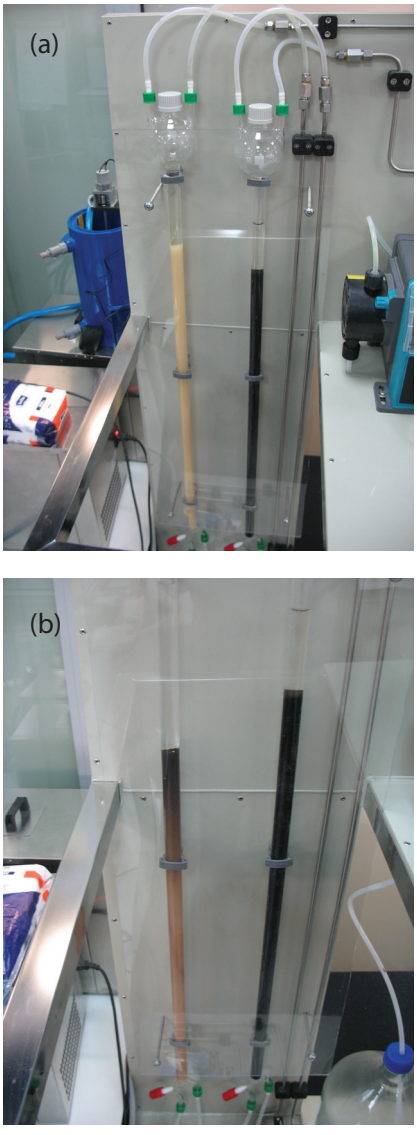

Fig. 3. Lewatit MonoPlus M 500 resin (left column on both pictures) before and after five service cycles.

Fig. 4. Lewatit S 5428 resin after five service cycles (left column).

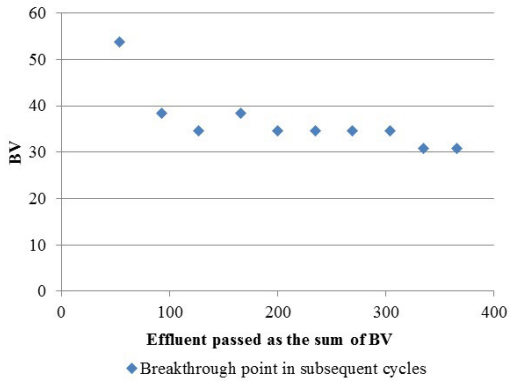

Fig. 5. Decrease of total capacity in the research conducted on Lewatit MonoPlus M 500 resin, BV – bed volume.

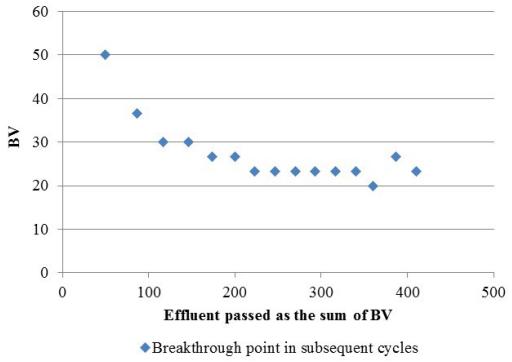

Fig. 6. Decrease of total capacity in the research conducted on Lewatit S 5428 resin, BV – bed volume.

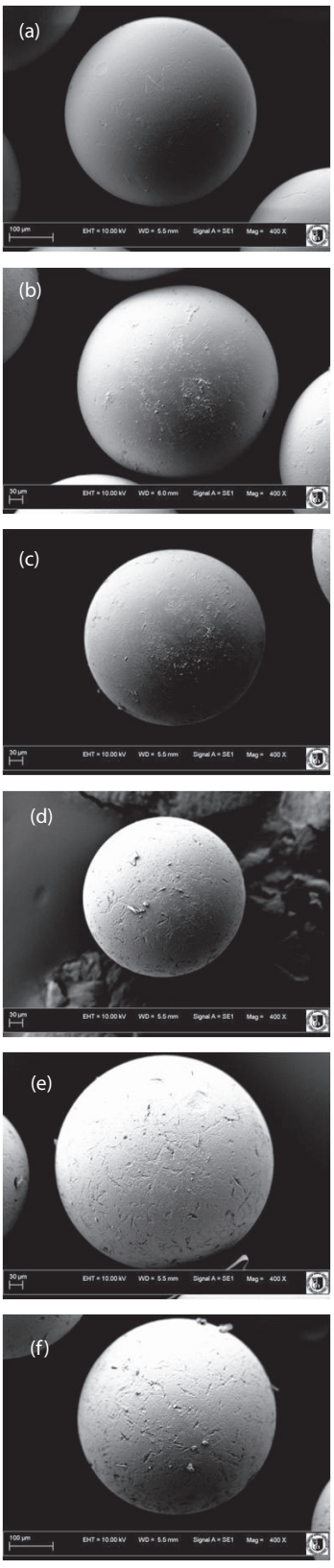

Fig. 7. SEM images of Lewatit Monoplus M 500: (a) fresh, (b) exhausted, and (c) regenerated bead, and Lewatit S 5428: (d) fresh, (e) exhausted, and (f) regenerated bead at 400× magnification.

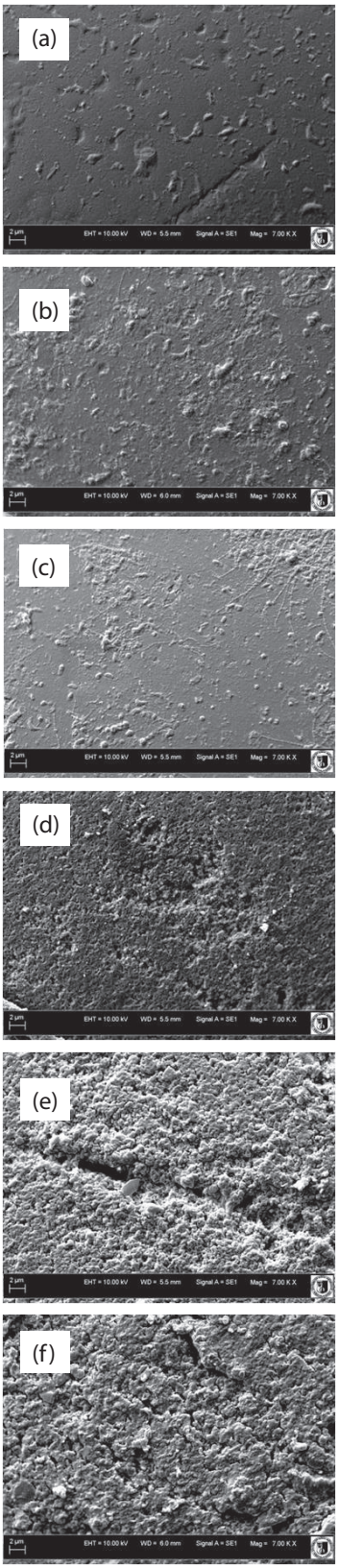

Fig. 8. SEM images of Lewatit Monoplus M 500: (a) fresh, (b) exhausted, and (c) regenerated bead, and Lewatit S 5428: (d) fresh, (e) exhausted, and (f) regenerated bead at 7,000× magnification.

respectively. Lewatit S 5428 is not a single particle size, but it is polydisperse resin, which explains different sizes of the beads on Fig. 7. On both figures the surface of the regenerated beads appeared different than the surface of the fresh ones and similar to the exhausted ones, which indicates the irreversible character of the accumulation of the compounds on the resins surface. Figs. 9 and 10 show the ATR-FTIR spectra of fresh, exhausted and regenerated beads of Lewatit MonoPlus M 500 and Lewatit S 5428, respectively. It could be observed that the spectra of exhausted and regenerated beads were characterised by the absorption bands at the same wavenumbers and differed from the spectra of fresh beads of Lewatit MonoPlus M 500 and Lewatit S 5428. Spectral subtraction of fresh bead spectrum from regenerated bead spectrum was performed in order to examine the surface of both anion exchangers after the regeneration. Fig. 11 shows the spectral subtraction for Lewatit MonoPlus M 500 and Fig. 12 – for Lewatit S 5428. The absorbance peaks at around 2,920–2,918 cm^{-1} and around 2,851–2,850 cm^{-1} most probably indicate the presence of aliphatic or alicyclic C–H stretching species. The peak at around 1,654 cm^{-1} indicates the existence of C=O stretching [33]. According to Wang et al. [34] and Maluf et al. [35] the strong absorption peak at 1,606 and 1,574 cm^{-1} can be assigned to the aromatic structures. The strong peak at 1,750 cm^{-1} indicates the existence of keto C=O or carboxyl C=O groups, and peak around 1,223 cm^{-1} is attributed to the C–O stretching vibration in phenol, ether or alcohol functional groups [34]. Therefore it is probable that the compounds adsorbed on the surface of the analysed resin beads contained aromatic structures with aliphatic side chains with keto, phenol or carboxyl groups. This confirms that HAs were accumulating on the beads of both ion exchangers and were present to a lesser or greater degree on the surface of the beads after regeneration.

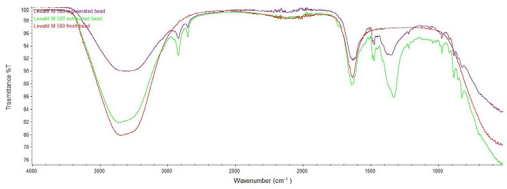

Fig. 9. FTIR spectra of fresh, exhausted, and regenerated Lewatit MonoPlus M 500 beads.

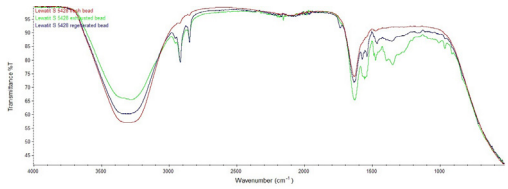

Fig. 10. FTIR spectra of fresh, exhausted, and regenerated Lewatit S 5428 beads.

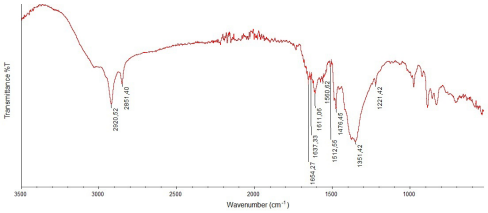

Fig. 11. FTIR spectrum obtained through the subtraction of fresh spectrum of Lewatit MonoPlus M 500 bead from the regenerated bead spectrum.

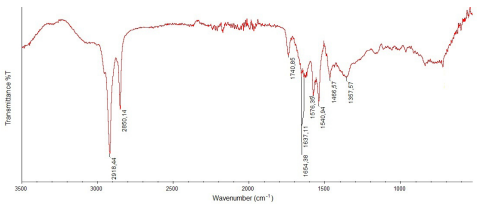

Fig. 12. FTIR spectrum obtained through the subtraction of fresh spectrum of Lewatit S 5428 bead from the regenerated bead spectrum.

Image analysis shows a two-dimensional image of three-dimensional particles, which serves as the basis for calculating various size and shape parameters. The main parameter is circle equivalent diameter, the diameter of a circle with the same area as the two-dimensional image of the particle. The diameter of this circle is treated as the diameter of the analysed particle [32,36]. Figs. 13 and 14 present the percentage share of equivalent beads, and Figs. 15 and 16 – high sensitive (HS) circularity of resin beads. Circularity is a parameter that informs how close the shape of the analysed particle approaches that of a circle. The circularity of the perfect circle is 1, while the circularity of narrow and elongated objects is close to 0.

It could be observed that fresh resin beads were smaller and more circular than the beads of resin after the last cycle

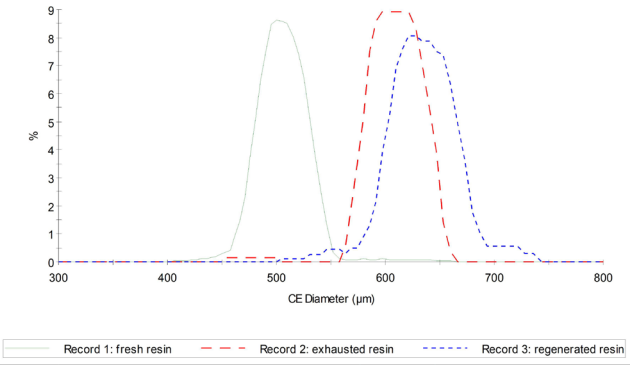

Fig. 13. Size distributions of Lewatit MonoPlus M 500 beads.

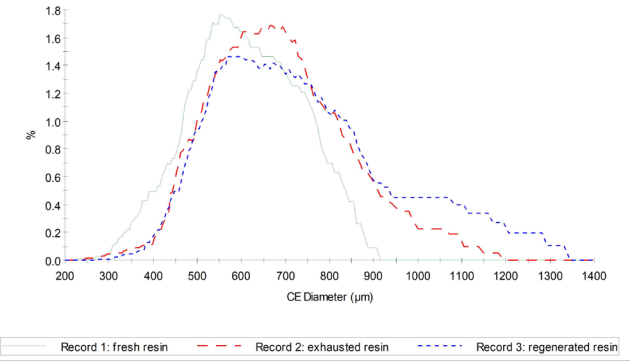

Fig. 14. Size distributions of Lewatit S 5428 beads.

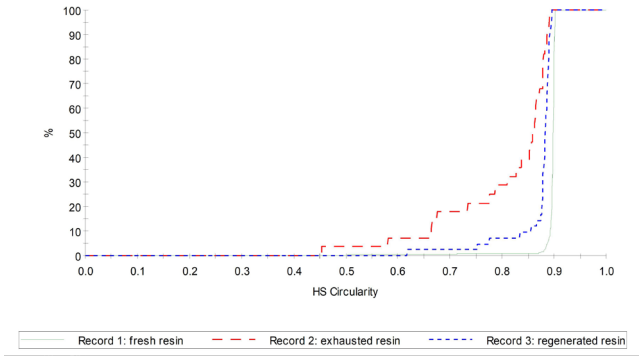

Fig. 15. HS circularity of Lewatit MonoPlus M 500 beads.

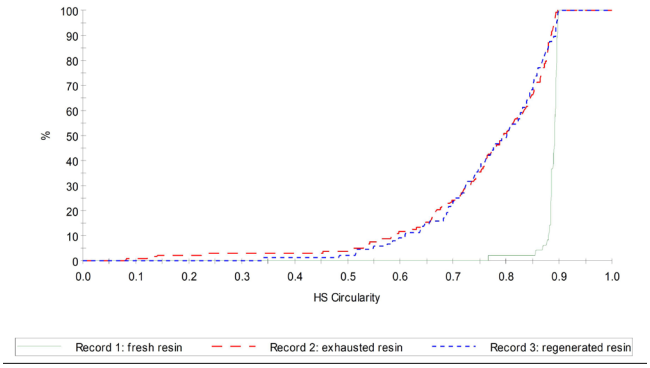

Fig. 16. HS circularity of Lewatit S 5428 beads.

of IE, both in the case of Lewatit MonoPlus M 500 and Lewatit S 5428 resins. The regeneration process resulted in an increase in the size of resin beads due to the phenomenon of expansion in the wake of the diffusion of mobile ions inside the beads. Regeneration caused an increase in the circularity of exhausted resin beads, which proves that chemical compounds adsorbed on the bead surface had been partially torn off. The change in the shape of the beads demonstrates the occurrence of resin ageing processes due to the adsorption of chemical compounds on the beads.

Figs. 17 and 18 show the results of the analysis of the width/length ratio (aspect ratio) in resin beads. In the case of the Lewatit MonoPlus M 500 and Lewatit S 5428 anion exchangers, the percentage of beads with a given aspect ratio was similar for the exhausted and the regenerated beads. Fresh beads of both anion exchangers used in the study were characterised by higher width/length ratios than exhausted beads. It proves that as a result of ageing processes, the beads of both resins changed their shapes from circular to oval.

Fig. 19 presents photographs of the Lewatit MonoPlus M 500 resin beads taken by the Malvern Morphologi G3SE analyser. The photographs depict a change occurring on the surface of the beads due to the accumulation of organic compounds. The device used in the study made it possible to determine the average of the pixel greyscale levels (intensity mean) of the beads surface on the basis of an analysis of the colour of pixels forming the beads surface. Intensity mean equal to 0 denotes black pixels, whereas level 255 corresponds to the white colour [32]. By analysing the graphs shown in Figs. 20 and 21 it was possible to determine that intensity

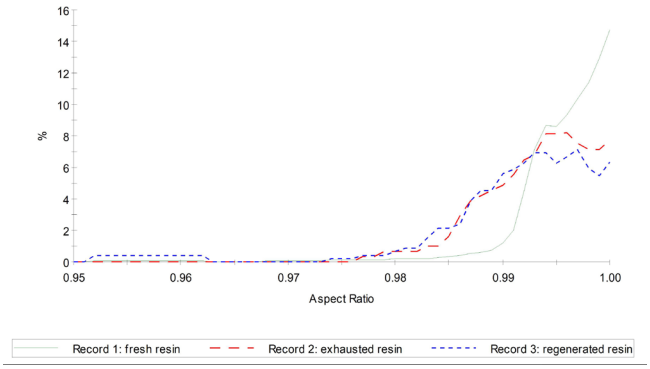

Fig. 17. Aspect ratio of Lewatit MonoPlus M 500 beads.

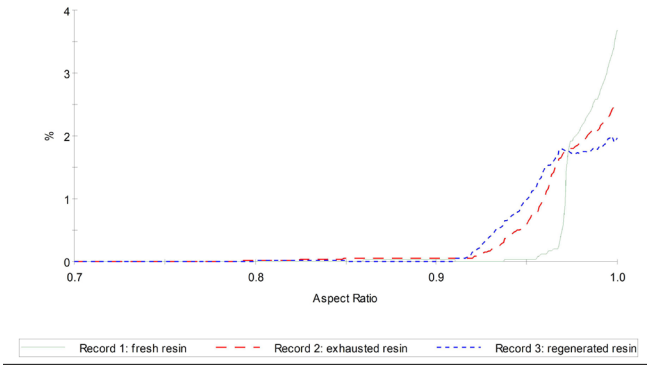

Fig. 18. Aspect ratio of Lewatit S 5428 beads.

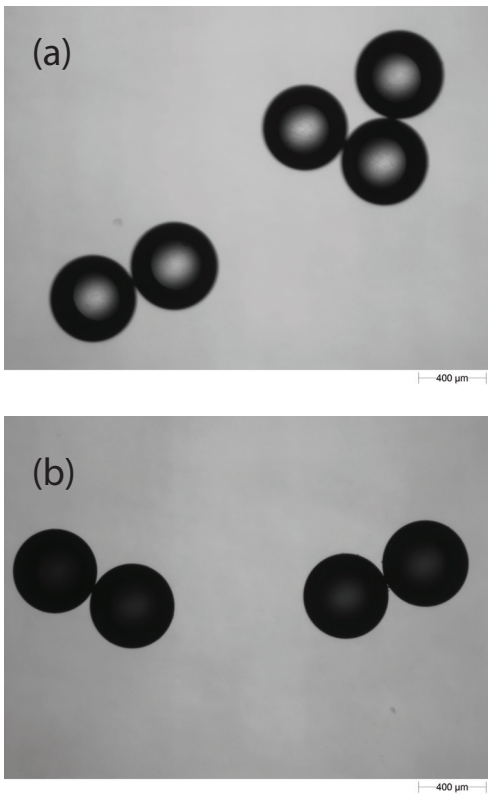

Fig. 19. Beads of Lewatit MonoPlus M 500: (a) fresh and (b) exhausted.

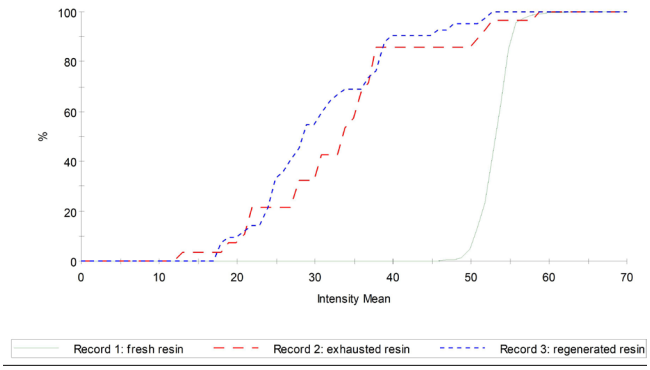

Fig. 20. Intensity mean of Lewatit MonoPlus M 500 beads.

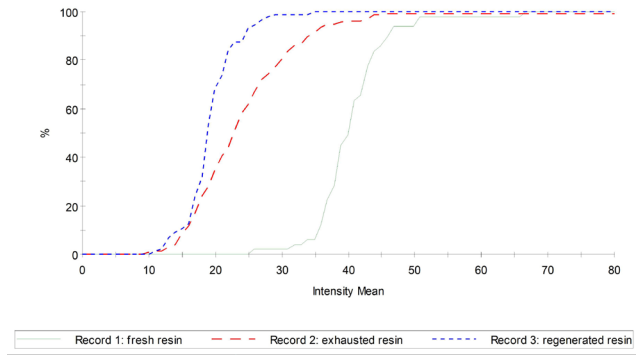

Fig. 21. Intensity mean of Lewatit S 5428 beads.

mean increased during the exploitation process in both resins. 90% of exhausted and regenerated Lewatit MonoPlus M 500 resin beads were characterised by intensity mean of 40 or higher, while all the fresh resin beads had intensity mean of between 45 and 60. About 60% of exhausted and about 90% of regenerated Lewatit S 5428 resin beads had intensity mean lower than 25, while all the fresh beads had intensity mean of more than 25.

The conducted research demonstrated the usefulness of the G3SE analyser, FTIR spectrometer and SEM for observing the ageing process of anion-exchange resins. By analysing the SEM images, FTIR spectra and the morphological parameters it was possible to determine the occurrence of a change in the shape and size of the beads of both anion exchangers during the IE process, which proved the ongoing ageing process. The accumulation of chemical compounds on the surface of anion exchangers beads was established by SEM and FTIR analyses of fresh, exhausted and regenerated beads of anion exchangers. It was demonstrated that HAs passed through NF membranes (flat and spiral) and accumulated irreversibly on the beads of both analysed resins during IE process. In the wake of the accumulation the beads shape changed from circular to more elongated.

4. Conclusions

- The conducted primarily research on the ageing process of strongly basic anion exchangers with the use of image analysis, SEM and FTIR spectroscopy made it possible to better understand the nature of this phenomenon. The aforementioned instrumental methods provide the additional knowledge on the resin surface changes which occur during the IE process.
- FTIR analysis of fresh, exhausted and regenerated resin beads showed the accumulation of HAs on the beads surface of both resins. The regeneration process proved to be ineffective, inasmuch as the HAs remained on the surface of regenerated beads.
- The performed image analysis showed that the accumulation of chemical compounds on the surface of anion exchangers beads resulted in the change of their size and shape. Resin regeneration removed compounds adsorbed on the surface only to a limited degree, which demonstrates the irreversible character of the process.
- It is necessary to conduct further research on the process of anion exchangers ageing with research instruments using image analysis, SEM and FTIR spectroscopy.

Acknowledgement

The research was financed by the National Centre for Research and Development as part of project no. PBS2/B9/25/2014.

References

[1] A. Kowal, M. Świderska-Bróż, Oczyszczanie wody, PWN, Warszawa, 2007.
[2] N.P. Cheremisinoff, Handbook of Water and Wastewater Treatment Technologies, Butterworth-Heinemann, Washington D.C., 2002.
[3] Z. Beril Gönder, Y. Kaya, I. Vergili, H. Barlas, Capacity loss in an organically fouled anion exchanger, Desalination, 189 (2006) 303–307.
[4] W.E. Bornak, R. Finley, F. Eckert, Method for Reducing Natural Organic Fouling Levels in a Contaminated Ion Exchange Resin, US Patent No. 7799228B2, 2010.
[5] H. Li, A. Li, C. Shuang, Q. Zhou, W. Li, Fouling of anion exchange resin by fluorescence analysis in advanced treatment of municipal wastewaters, Water Res., 66 (2014) 233–241.
[6] A.S. Koparal, Y.S. Yildiz, B. Keskinler, N. Demircioğlu, Effect of initial pH on the removal of humic substances from wastewater by electrocoagulation, Sep. Purif. Technol., 59 (2008) 175–182.
[7] F.J. DeSilva, Removing organics with ion exchange resin, Water Condit. Purif. Mag., (1997) 1–3.
[8] J.N. Wang, A.M. Li, Y. Zhou, L. Xu, Study on the influence of humic acid of different molecular weight on basic ion exchange resin's adsorption capacity, Chin. Chem. Lett., 20 (2009) 1478–1482.
[9] D. Kliaugaitė, K. Yasadi, G. Euverink, M.F.M. Bijmans, V. Racys, Electrochemical removal and recovery of humic-like substances from wastewater, Sep. Purif. Technol., 108 (2013) 37–44.
[10] J. Kaleta, Humus substances in water medium, Zeszyty Naukowe Politechniki Rzeszowskiej Budownictwo i Inżynieria Środowiska, 38 (2004) 39–53.
[11] G.-C. Lee, G.L. Foutch, A. Arunachalam, An evaluation of mass-transfer coefficients for new and used ion-exchange resins, React. Funct. Polym., 35 (1997) 55–73.
[12] Y. Tan, J.E. Kilduff, Factors affecting selectivity during dissolved organic matter removal by anion-exchange resins, Water Res., 41 (2007) 4211–4221.
[13] M. Kabsch-Korbutowicz, Application of ion exchange to natural organic matter removal from water, Ochrona Srodowiska, 35 (2013) 11–18.
[14] S.K. Zheng, J.J. Chen, X.M. Jiang, X.F. Li, A comprehensive assessment on commercially available standard anion resins for tertiary treatment of municipal wastewater, Chem. Eng. J., 169 (2011) 194–199.

[15] F. de Dardel, T.V. Arden, Ion Exchangers. Principles and Applications, Wiley-Vch, Germany, 2001.
[16] M. Chabani, A. Amrane, A. Bensmaili, Kinetics of nitrates adsorption on Amberlite IRA 400 resin, Desalination, 206 (2007) 560–567.
[17] E. Pehlivan, S. Cetin, Sorption of Cr(VI) ions on two Lewatit-anion exchange resins and their quantitative determination using UV–visible spectrophotometer, J. Hazard. Mater., 163 (2009) 448–453.
[18] J.B. de Heredia, J.R. Domínguez, Y. Cano, I. Jiménez, Nitrate removal from groundwater using Amberlite IRN-78: modelling the system, Appl. Surf. Sci., 252 (2006) 6031–6035.
[19] K.M. Walker, T.H. Boyer, Long-term performance of bicarbonate-form anion exchange: removal of dissolved organic matter and bromide from the St. Johns River, FL, USA, Water Res., 45 (2011) 2875–2886.
[20] M. Wawrzkiewicz, Z. Hubicki, Kinetic studies of dyes sorption from aqueous solutions onto the strongly basic anion-exchanger Lewatit MonoPlus M-600, Chem. Eng. J., 150 (2009) 509–515.
[21] L. Benavente, C. Coetsier, A.Venault, Y. Chang, C. Causserand, P. Bacchin, P. Aimar, FTIR mapping as a simple and powerful approach to study membrane coating and fouling, J. Membr. Sci., 520 (2016) 477–489.
[22] O. Thygesen, M.A.B. Hedegaard, A. Zarebska, C. Beleites, C. Krafft, Membrane fouling from ammonia recovery analyzed by ATR-FTIR imaging, Vib. Spectrosc., 72 (2014) 119–123.
[23] H. Li, Y. Lin, P. Yu, Y. Luo, L. Hou, FTIR study of fatty acid fouling of reverse osmosis membranes: effects of pH, ionic strength, calcium, magnesium and temperature, Sep. Purif. Technol., 77 (2011) 171–178.
[24] M. Bass, V. Freger, Facile evaluation of coating thickness on membranes using ATR-FTIR, J. Membr. Sci., 492 (2015) 348–354.
[25] S. Belfer, J. Gilron, O. Kedem, Characterization of commercial RO and UF modified and fouled membranes by means of ATR/FTIR, Desalination, 124 (1999) 175–180.
[26] M. Palencia, T. Lerma, V. Palencia, Description of fouling, surface changes and heterogeneity of membranes by color-based digital image analysis, J. Membr. Sci., 510 (2016) 229–237.
[27] K.-L. Tung, H.-C. Teoh, C.-W. Lee, C.-H. Chen, Y.-L. Li, Y.-F. Lin, C.-L. Chen, M.-S. Huang, Characterization of membrane fouling distribution in a spiral wound module using high-frequency ultrasound image analysis, J. Membr. Sci., 495 (2015) 489–501.
[28] K. Xiao, F. Xu, L. Jiang, N. Duan, S. Zheng, Resin oxidization phenomenon and its influence factor during chromium(VI) removal from wastewater using gel-type anion exchangers, Chem. Eng. J., 283 (2016) 1349–1356.
[29] S. Addepalli, Industrial applications of X-ray photoelectron spectroscopy (XPS) in India, J. Electron. Spectrosc. Relat. Phenom., (2018). doi: 10.1016/j.elspec.2018.05.002.
[30] C.A. Rokicki, T.H. Boyer, Bicarbonate-form anion exchange: affinity, regeneration and stoichiometry, Water Res., 45 (2011) 1329–1337.
[31] L. Jelinek, H. Parschova, Z. Matejka, M. Paidar, K. Bouzek, A combination of ion exchange and electrochemical reduction for nitrate removal from drinking water. Part I: nitrate removal using a selective anion exchanger in the bicarbonate form with reuse of the regenerant solution, Water Environ. Res., 76 (2004) 2686–2690.
[32] Morphologi G3 User Manual: MAN0410-07-EN-00, Malvern Instruments Ltd., England, 2015.
[33] X. Zhang, B. Pan, K. Yang, D. Zhang, J.A. Hou, Adsorption of sulfamethoxazole on different types of carbon nanotubes in comparison to other natural adsorbents, J. Environ. Sci. Health Part A, 45 (2010) 1625–1634.
[34] C.-F. Wang, X. Fan, F. Zhang, S.-Z. Wang, Y.-P. Zhao, X.-Y. Zhao, W. Zhao, T.-G. Zhu, J.-L. Luc, X.-Y. Wei, Characterization of humic acids extracted from a lignite and interpretation for the mass spectra, RSC. Adv., 7 (2017) 20677–20684.
[35] H.J.G.M. Maluf, C.A. Silva, N. Curi, L.D. Norton, S.D. Rosa, Adsorption and availability of phosphorus in response to humic acid rates in soils limed with $CaCO_3$ or $MgCO_3$, Cienc. Agrotechnol., 42 (2018) 7–20.
[36] U. Willen, Extending Particle Characterization: Automation in Image Analysis for Size and Shape Management, Analytical and Bioscience Solutions Update, 12–14, Malvern Instruments, MRK1075, 2008.